Available online at www.sciencedirect.com
SCIENCE DIRECT®
Polymer 44 (2003) 7209–7220
polymer
www.elsevier.com/locate/polymer

Determination of molecular weight and molecular sizes of polymers by high temperature gel permeation chromatography with a static and dynamic laser light scattering detector

Yonggang Liu, Shuqin Bo*, Yejuan Zhu, Wenhe Zhang

State Key Laboratory of Polymer Physics and Chemistry, Changchun Institute of Applied Chemistry, Chinese Academy of Sciences, Changchun 130022, People's Republic of China

Received 7 April 2003; received in revised form 5 August 2003; accepted 7 August 2003

Abstract

Flow-mode static and dynamic laser light scattering (SLS/DLS) studies of polymers, including polystyrene, polyethylene, polypropylene and poly(dimethylsiloxane) (PDMS), in 1,2,4-trichlorobenzene (TCB) at 150 °C were performed on a high temperature gel permeation chromatography (GPC) coupled with a SLS/DLS detector. Both absolute molecular weight (M) and molecular sizes (radius of gyration, R_g and hydrodynamic radius, R_h) of polymers eluting from the GPC columns were obtained simultaneously. The conformation of different polymers in TCB at 150 °C were discussed according to the scaling relationships between R_g, R_h and M and the ρ-ratio ($\rho = R_g/R_h$). Flow-mode DLS results of PDMS were verified by batch-mode DLS study of the same sample. The presented technique was proved to be a convenient and quick method to study the shape and conformation of polymers in solution at high temperature. However, the flow-mode DLS was only applicable for high molecular weight polymers with a higher refractive index increment such as PDMS.

Keywords: Gel permeation chromatography; Static light scattering; Dynamic light scattering

1. Introduction

Gel permeation chromatography (GPC or size exclusion chromatography, SEC) coupled with a low angle Rayleigh or static laser light scattering (LALLS) detector has long been used to determine the absolute molecular weight (M) and molecular weight distribution (MWD) of polymers [1]. When a two-angle laser light scattering (TALLS) or multi-angle laser light scattering (MALLS) detector is connected to a GPC system, radius of gyration (R_g) as a function of molecular weight of polymers can be obtained [2,3]. Dynamic laser light scattering (DLS) had long been used to determine the hydrodynamic radius (R_h) of polymers in batch-mode [4,5]. Recent innovations in modern high-speed electronic components such as high-performance diode lasers, high-speed digital signal processors and modern avalanche photodiode detectors have led to the evolution of a new flow-mode DLS detector, which had been used for 'on-the-fly' determination of R_h of biomolecules eluting from the SEC columns [6]. The combination of static and dynamic light scattering detector is capable of characterizing both absolute M and molecular sizes (R_g, R_h) for polymers eluting from modern GPC/SEC instruments. Further, the relationships between R_g, R_h and M of polymers and the ρ-ratio ($\rho = R_g/R_h$) are obtained, which provide information on molecular shape and conformation of polymers in solution. However, few results of flow-mode DLS studies of polymers in GPC have been reported in the literatures, especially in high temperature GPC.

In this study, a high temperature GPC coupled with a TALLS/DLS detector (GPC-TALLS/DLS) was used to simultaneously determine the molecular weight and molecular sizes (R_g, R_h) of polymers. It was proved to be a convenient and quick method to study the shape and conformation of polymers in solution at high temperature.

* Corresponding author. Tel.: +86-431-5262130; fax: +86-431-5262126.
E-mail addresses: ygliu@ns.ciac.jl.cn (Y. Liu), sqbo@ns.ciac.jl.cn (S. Bo).

0032-3861/$ - see front matter © 2003 Elsevier Ltd. All rights reserved.
doi:10.1016/j.polymer.2003.08.037

2. Theoretical background

The static laser light scattering (SLS) detectors measure excess Rayleigh scattering $R_{\theta i}$ at angle θ for each retention volume V_i at a GPC chromatogram. This scattering intensity is related to the concentration at each retention volume, C_i, which is measured by a separated concentration-sensitive (e.g. differential refractive index or DRI) detector:

$$\frac{KC_i}{R_{\theta i}} = \frac{1}{M_{wi}P(\theta)_i} + 2A_{2i}C_i + \cdots \quad (1)$$

The particle scattering function $P(\theta)_i$ defines the angular variation of scattering intensity. M_{wi} is the molecular weight at retention volume V_i and is a weight-average if the slice contains molecules of more than one molecular weight. A_{2i} is the second virial coefficient at retention volume V_i and K is an optical constant.

The second and higher concentration terms of Eq. (1) are usually negligible at the low polymer concentrations employed in GPC. In this case,

$$M_{wi} \approx \frac{R_{\theta i}}{KC_iP(\theta)_i} \quad (2)$$

At low angle, the particle scattering function approaches unity even for large molecular size. This simplifies the calculation of molecular weight by LALLS in which scattering intensity are measured at observation angle of 7° or less [1]. Accurate molecular weight can be measured, but no information on molecular size is obtained from light scattering intensity at a single low angle. MALLS instruments that collect light scattered by polymer molecules at multiple, higher angles of observation measures scattering intensities for which $P(\theta) \neq 1$. The scattering data are extrapolated to zero angle to obtain molecular weight, M_{wi} and molecular size, R_{gi} [3].

However, the classical extrapolating method cannot be applied to the data obtained at only two angles. In fact, an alternative method was described for TALLS detector in the literature [2,7]. The ratio of the scattering intensities, Z_i, at two angles θ_1 and θ_2, are measured. It is directly proportional to the ratio of particle scattering function at the same two angles:

$$Z_i = \frac{R_{\theta_1 i}}{R_{\theta_2 i}} = \frac{P(\theta_1)_i}{P(\theta_2)_i} \quad (3)$$

Values of R_{gi} and $P(\theta)_i$ (and then M_{wi}) for a given Z_i can be calculated by assuming a particle scattering function (e.g. random coil) and by iteration suggested by Mourey, et al. [2], or using the series expressions suggested by Ford, et al. [7]. Their studies had showed that accurate and precise M_w and $R_{g,z}$ were obtained for polystyrene in tetrahydrofuran at room temperature. The latter was included in the commercial Discovery32 software (Precision Detectors Inc.).

DLS measures the scattering light intensity fluctuation and records an intensity–intensity time correlation function $G^{(2)}(t)$, which is related to the normalized electric field time correlation function $g^{(1)}(t)$ by [4]

$$G^{(2)}(t) = \langle I(0)I(t)\rangle = A(1 + \beta|g^{(1)}(t)|^2) \quad (4)$$

where A is the measured baseline, β is a parameter depending on the coherence of the detection optics, and t is the delay time.

For a monodisperse sample, $|g^{(1)}(t)|$ is theoretically represented by an exponentially decaying function

$$|g^{(1)}(t)| = \exp(-\Gamma t) \quad (5)$$

where Γ is the line-width, which related with the apparent transitional diffusion coefficient D_{app} as

$$\Gamma = q^2 D_{app} \quad (6)$$

For dilute solution, D_{app} measured at a finite scattering angle is related to sample concentration C and scattering angle θ by

$$D_{app} = D(1 + k_dC)(1 + fR_g^2q^2) \quad (7)$$

where $q = (4\pi n/\lambda_0)\sin(\theta/2)$ with n, λ_0 being the solvent refractive index and the wavelength of light in vacuum, respectively. D is the transitional diffusion coefficient at $C \to 0$ and $\theta \to 0$, k_d is the diffusion second virial coefficient, f is a dimensionless number with a typical value between 0.1 and 0.2 [8–10].

In the flow-mode DLS experiments, the intensity–intensity time correlation function is accumulated for sample eluting from the GPC columns, which is nearly monodisperse. The concentration of the eluted sample is very low (with a typical magnitude of 0.1 mg/ml) and thus the dependence of D_{app} on C can be neglected. In this case

$$D_{app} \approx D(1 + fR_g^2q^2) \quad (8)$$

The transitional diffusion coefficient D is related to hydrodynamic radius R_h according to the Stokes–Einstein equation:

$$D = \frac{k_BT}{6\pi\eta_0R_h} \quad (9)$$

where k_B, T and η_0 are the Boltzmann constant, absolute temperature and solvent viscosity, respectively.

An apparent hydrodynamic radius $R_{h,app}$ can be calculated from D_{app} by

$$R_{h,app} = \frac{k_BT}{6\pi\eta_0D_{app}} \quad (10)$$

Fortunately, the radius of gyration R_g of the sample can be determined by TALLS as it eluted through the same flow cell, which had been described as above. Then D can be calculated according to Eq. (8) with an assumption of f. And R_h of the sample can be calculated from D according to Eq. (9):

$$R_h = \frac{k_BT}{6\pi\eta_0D} = R_{h,app}(1 + fR_g^2q^2) \quad (11)$$

A number of f values had been theoretically calculated or experimentally determined [8–10]. To obtain a correct R_h, it is very important to assume an appropriate value of f, especially for a large size sample.

Once the concentration C_i, molecular weight M_{wi} and molecular size (R_{gi} and R_{hi}) at each retention volume V_i along the entire GPC chromatogram have been determined, their average properties can be calculated as follows:

Number-average molecular weight

$$M_n = \frac{\sum C_i}{\sum C_i M_{wi}^{-1}} \tag{12}$$

Weight-average molecular weight

$$M_w = \frac{\sum C_i M_{wi}}{\sum C_i} \tag{13}$$

z-average molecular weight

$$M_z = \frac{\sum C_i M_{wi}^2}{\sum C_i M_{wi}} \tag{14}$$

Number-average radius of gyration

$$R_{gn} = \left(\frac{\sum C_i M_{wi}^{-1} R_{gi}^2}{\sum C_i M_{wi}^{-1}} \right)^{1/2} \tag{15}$$

Weight-average radius of gyration

$$R_{gw} = \left(\frac{\sum C_i R_{gi}^2}{\sum C_i} \right)^{1/2} \tag{16}$$

z-average radius of gyration

$$R_{gz} = \left(\frac{\sum C_i M_{wi} R_{gi}^2}{\sum C_i M_{wi}} \right)^{1/2} \tag{17}$$

The z-average hydrodynamic radius is defined as [10]

$$\left(\left\langle \frac{1}{R_h} \right\rangle_z \right)^{-1} = \frac{\sum C_i M_{wi}}{\sum C_i M_{wi} R_{hi}^{-1}} \tag{18}$$

Similarly, the number-average and weight-average hydrodynamic radius can be defined as

$$\left(\left\langle \frac{1}{R_h} \right\rangle_n \right)^{-1} = \frac{\sum C_i M_{wi}^{-1}}{\sum C_i M_{wi}^{-1} R_{hi}^{-1}} \tag{19}$$

$$\left(\left\langle \frac{1}{R_h} \right\rangle_w \right)^{-1} = \frac{\sum C_i}{\sum C_i R_{hi}^{-1}} \tag{20}$$

They were abbreviated to R_{hz}, R_{hn} and R_{hw}, respectively, in this study.

3. Experimental

3.1. GPC-TALLS/DLS

A PL-GPC 220 high temperature gel permeation chromatography (Polymer Laboratories Ltd.) coupled with an online PD2040/DLS laser light scattering detector (Precision Detectors Inc.) was used in this study. The columns used were three PLgel 10 μm Mixed-B LS columns (300 × 7.5 mm). The eluent was 1,2,4-trichlorobenzene (TCB, Acros) stabilized with 5×10^{-4} g/ml 2,6-di-*tert*-butyl-4-methylphenol (BHT, Acros) and was filtered with a 0.2 μm pore size membrane before use. The injection volume was 200 μl and the flow rate was 1.0 ml/min. All measurements were performed at 150 °C.

The PD2040/DLS detector, which contained two angle (15 and 90°) SLS detectors and one angle (90°) DLS detector, was positioned before the differential refractive index (DRI) detector. A 30 mW, 680 nm semiconductor diode laser light source was used. Its flow cell, with a volume of 10 μl and a very small optical volume of less than 0.01 μl, was located in the GPC oven.

The TALLS and the DRI detector were calibrated by multiple injection of a narrow distribution polystyrene (PS) standard with $M_w = 21$ k and $M_w/M_n = 1.02$. The inter-detector volume between the TALLS/DLS detector and the DRI detector was also determined by this PS standard by superimposing the onsets of the TALLS and the DRI responses.

The columns were also calibrated with EasiCal® PS-1 standard (PL Ltd.) and some individual narrow PS standards (Polyscience Inc. and PL Ltd.), which were injected with concentrations ranging from 0.5 to 2.5 mg/ml, depending on molecular weight.

Some broad samples were run to show the possible application of the method, which were: two homemade broad PS samples (PS600k, PS4M), a commercial high-density polyethylene (HDPE) resin, a commercial polypropylene (PP) resin and a commercial poly(dimethylsiloxane) (PDMS) sample.

All sample solutions were prepared using PL-SP 260 high temperature sample preparation system (PL Ltd.) at 150 °C. The solution was filtered with a 2 μm frit after keeping for 2–4 h at 150 °C.

The refractive index increment, dn/dc of the samples were determined by the calibrated DRI detector. In this study, a value of 0.053 ml/g for dn/dc of PS in TCB at 150 °C was assumed and $dn/dc = -0.097$ ml/g for PE and PP were calculated, which agreed with the values in the literature within experimental error [1]. For PDMS, $dn/dc = -0.153$ ml/g was obtained.

PrecisionAcquire32 software from Precision Detectors Inc. was used to acquire data from the TALLS/DLS detector and the DRI detector in 1 s intervals. The acquired data were processed with Discovery32 software (Precision Detectors Inc.) to obtain M_{wi} and R_{gi} of polymer for each elution slice.

Since a broad sample runs through the GPC columns and the TALLS/DLS detector in a few minutes, a proper accumulation time must be selected for DLS detector to provide accurate determination of the time correlation function as well as avoid detecting a mixture of the separated fractions from GPC columns. A typical accumulation

time used in this study is 10 s with 5 μs sampling time for the flow-mode DLS detector. That is to say, $R_{h,app}$ determined at each slice actually represented the samples eluted in 10 s.

The obtained M_{wi}, R_{gi} and $R_{h,app}$ as functions of retention volume (V_R) were exported to ASCII files and were further analyzed using Origin software.

3.2. Stop-flow GPC-TALLS/DLS and batch-mode DLS

In order to study the precision and accuracy of the results obtained in flow-mode DLS, the eluent flow was stopped at a special time after the sample entered the LS flow cell, then time correlation function was accumulated for a longer time, thus the flow-mode DLS detector served as a traditional batch-mode DLS detector. The time correlation function was collected and deconvolved by PrecisionDeconvolve software (Precision Detectors Inc.) to obtain D_{app} and $R_{h,app}$. The accumulation time was set to be 10, 60 and 600 s, respectively.

4. Results and discussion

4.1. PS

Fig. 1 showed a typical plot of the GPC-TALLS chromatograms of PS600k in TCB at 150 °C (with an injected concentration $C_{inj} = 2.47$ mg/ml). The SLS signal, which scales with the product of C and M, exhibits much greater intensity in the high M region, relative to the DRI response, which scales only with C. In addition, the scattering intensity of the 15° scattering angle is larger than that of the 90° scattering angle, indicating the angular dissymmetry of the scattering intensity of macromolecules, which is used to calculate R_{gi}, $P(\theta)_i$ and then M_{wi} at each elution slice.

Logarithms of M and R_g as functions of V_R for PS600k in TCB at 150 °C were shown in Fig. 2. Both logarithms of M

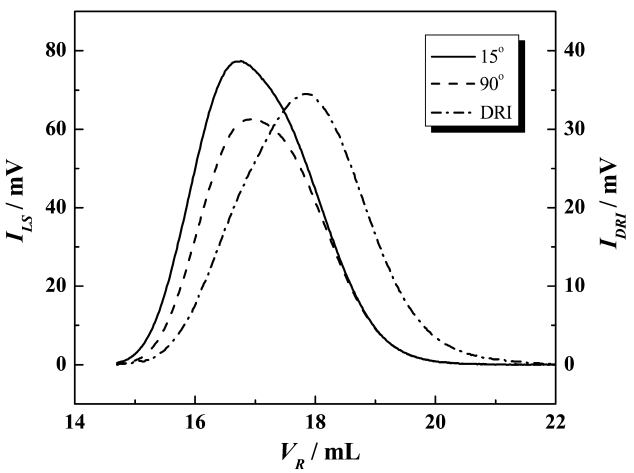

Fig. 1. GPC-TALLS chromatograms of PS600k in TCB at 150 °C.

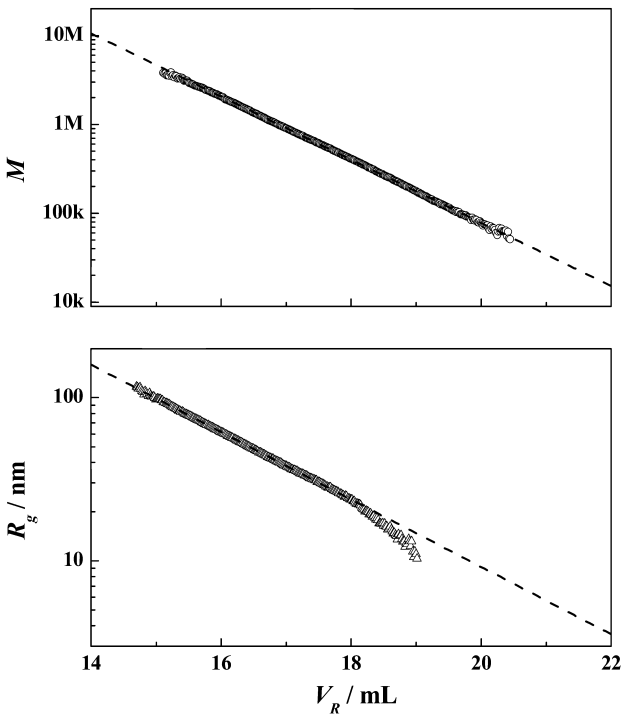

Fig. 2. Logarithms of M and R_g as functions of V_R for PS600k in TCB at 150 °C.

and R_g decreased linearly with increasing V_R, except a few deviations at both ends due to low signal-to-noise ratio in this region. It should be noted that the linear region of $M-V_R$ plot and R_g-V_R plot were different. The linear region of $M-V_R$ plot was close to the region of DRI response, while the linear region of R_g-V_R plot was close to the region of SLS response. Since determination of M requires knowing the polymer concentration, the low DRI signal at low V_R sets the high M limit, while determination of R_g requires the ratio of the scattering intensity at two angles, the much greater SLS signals in low V_R enable R_g to be accurately determined. On the other hand, at high V_R, the scattering intensity difference between the two angles is so little that R_g can't be accurately determined, while the DRI signal is still strong enough to obtain an accurate M. The absolute calibration curves of M and R_g for PS600k were established by lineally regression of the middle section of the data points and extrapolation to both ends. The absolute M and R_g distributions of PS600k were obtained using these calibration curves and the DRI response, as presented in Fig. 3. The different M and R_g averages were then calculated from these distributions according to Eqs. (12–14) and Eqs. (15–17), respectively.

The M averages thus calculated for 9 narrow PS standards and 2 broad PS samples were summarized in Table 1. For comparison with the traditional GPC with only DRI detector, the columns were also calibrated with EasiCal® PS-1, which contains 10 narrow PS standards with molecular weight ranging from 580 to 7.50 M. The M averages of the above PS samples were calculated from this

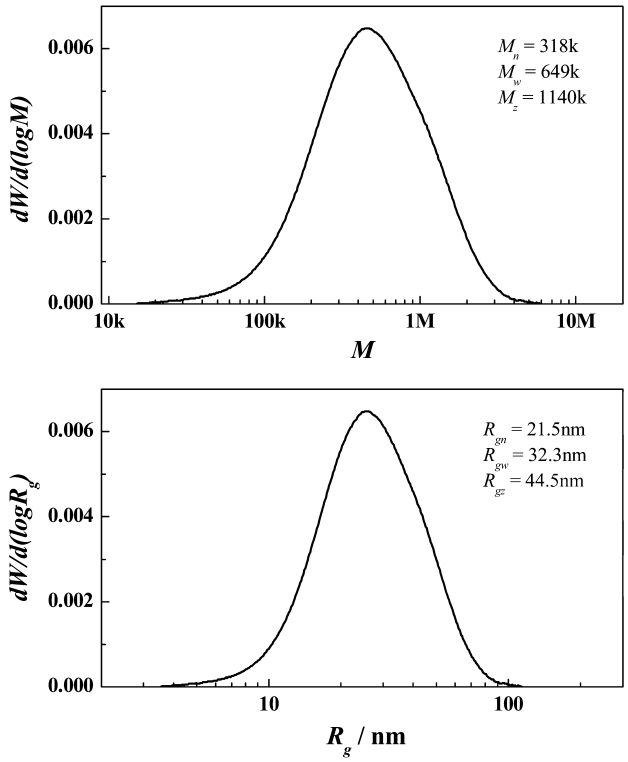

Fig. 3. Absolute M and R_g distributions of PS600k.

calibration curve and the DRI response and the results were also listed in Table 1. It is observed that the results obtained from GPC with or without TALLS detector are close, except that the inhomogeneity index M_w/M_n calculated from GPC with TALLS is lower than that calculated from GPC alone. It should be noted that M_{wi} for each slice obtained from TALLS is an absolute value and the calculated M_w is a true value despite the column dispersion, while a higher M_n and thus a lower M_w/M_n are obtained due to the column dispersion as had been discussed before by Cheng et al. [11]. On the other hand, GPC alone gives a higher M_w and a lower M_n, resulting a higher M_w/M_n, which is also due to the column dispersion. The true M_w/M_n is a value between them, which will be the subject of another work. It should also be noted that M_w calculated from GPC alone were only slightly higher than those calculated with TALLS, indicating that the column dispersion effect is low since high performance GPC columns were used in this study. In addition, the calculated molecular weight of some PS standards, which were purchased years before, differed a lot from those given by supplier, while the new PS standards agreed well. It indicated that some old PS standards must be examined carefully before use to calibrate the columns.

Table 1
M averages of PS samples

M[a] (k)	GPC-TALLS[b]			GPC-DRI[c]		
	M_w (k)	M_n (k)	M_w/M_n	M_w (k)	M_n (k)	M_w/M_n
7110	5720	5270	1.09	6210	4900	1.27
1920	1660	1640	1.01	1720	1520	1.13
390	404	401	1.01	417	377	1.11
233	267	265	1.01	260	238	1.09
218.8	223	221	1.01	223	203	1.10
92.6	98.8	98.3	1.01	100	93.2	1.07
110	91.0	88.4	1.03	90.3	72.9	1.24
65.0	66.9	66.4	1.01	69.3	64.1	1.08
21.0	21.4	21.2	1.01	22.0	20.3	1.08
4000[d]	4540	2680	1.69	4610	2270	2.03
600[e]	649	318	2.04	648	265	2.45

[a] Molecular weight of PS standards as given by supplier.
[b] Molecular weight of PS samples as determined by GPC-TALLS.
[c] Molecular weight of PS samples as determined by GPC with only DRI detector.
[d] PS4M with a broad MWD.
[e] PS600k with a broad MWD.

Fig. 4 showed the logarithm of M as a function of V_R for PS4M and PS600k, the calibration curve determined from EasiCal® PS-1 and the calculated M_w versus peak V_R of the narrow PS standards were also shown. The $M_w - V_R$ plot of the narrow PS standards calculated from GPC-TALLS was exactly on the calibration curve of EasiCal® PS-1, indicating the M_w calculated from GPC-TALLS for these narrow PS standards were correct. However, the $M - V_R$ plot of the broad PS samples, PS4M and PS600k, which was determined by GPC-TALLS at each retention volume, did not superpose on the calibration curve of EasiCal® PS-1. The former had a lower slope than the latter, which was due to the column dispersion [11]. Consequently, M_w/M_n calculated from GPC-TALLS had a lower value than that calculated from GPC, as the results shown in Table 1.

Similarly, the logarithm of R_g versus V_R curve of the broad PS samples, PS4M and PS600k, which was determined by GPC-TALLS at each retention volume, also had a lower slope due to the column dispersion, than the calibration curve of EasiCal® PS-1 (Fig. 5), which was calculated according to the relationship $R_g(\text{nm}) = 0.0138\,M^{0.58}$ from its molecular weight [12]. R_{gu}, which was calculated

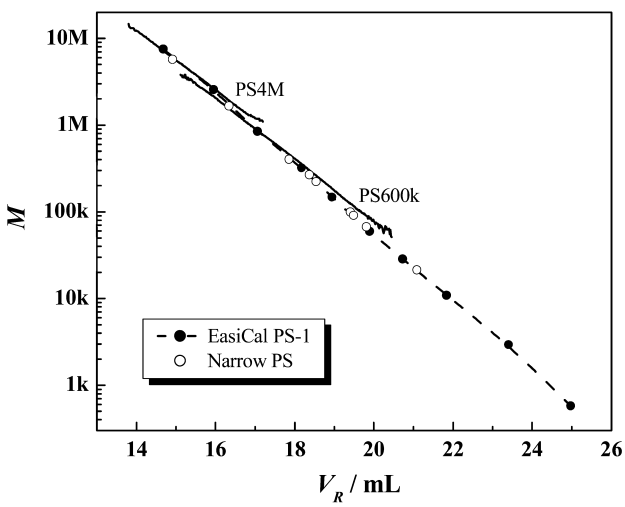

Fig. 4. Logarithm of M as a function of V_R for PS4M and PS600k.

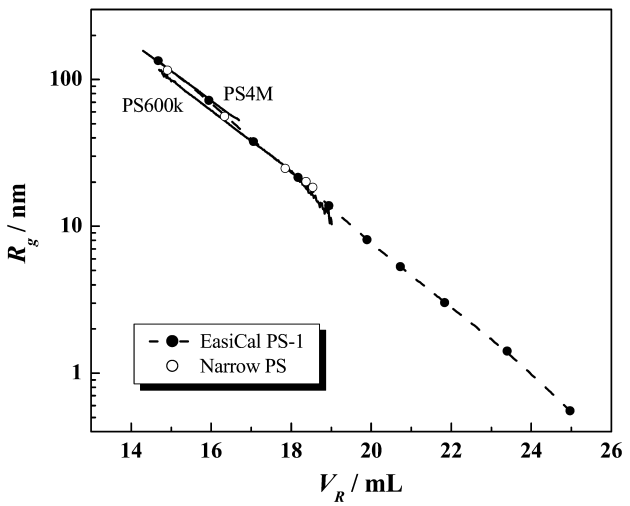

Fig. 5. Logarithm of R_g as a function of V_R for PS4M and PS600k.

from the ratio of the area under the chromatograms of two LS angles and was proved to be close to its R_{gz} [2], of the narrow PS standards were also shown. The narrow PS standards with R_{gu} larger than 18 nm superposed on the calibration curve of EasiCal® PS-1, while R_{gu} of those PS with M_w less than 100 k ($R_g < 10$ nm) couldn't be accurately determined by this detector due to the little difference between the scattering intensities at two angles for small molecules.

The accuracy of the determined R_{gu} for the narrow PS standards was examined by compare the $R_{gu}-M_w$ relationship with the literature data, as shown in Fig. 6. It agreed well with the data obtained by Ommundsen et al. [12] for PS standards with M_w larger than 200 k.

As we had indicated above, the high performance columns used here ensured a very narrow distribution in both molecular weight and molecular sizes for each elution slice. In addition, both molecular weight and molecular size determined by the TALLS detector at each V_R were absolute values. Consequently, the obtained scaling relationship between R_g and M ($R_g(\text{nm}) = 0.0118\,M^{0.59}$) can be considered as that of a homogeneous (monodisperse) system, as shown in Fig. 7. Unlike the different line for PS4M and PS600k in $M-V_R$ (Fig. 4) or R_g-V_R plot (Fig. 5), the R_g-M plot for PS4M and PS600k superposed into a same line, indicating that the true R_g-M relationship can still be obtained despite the column dispersion. The result obtained from narrow PS standards (Fig. 6) is very close to the scaling relationship. In addition, the scaling relationship had an exponent of 0.59, close to the theoretical value for random coil in good solvent [10,13], indicating that PS took a random coil conformation in TCB, a good solvent, at 150 °C.

4.2. PE and PP

Fig. 8 showed a typical plot of the GPC-TALLS chromatograms of PP in TCB at 150 °C (with $C_{inj} = 2.24$ mg/ml). Similar to the GPC-TALLS chromatograms of PS600k (Fig. 1), the SLS signal exhibits much greater intensity in the high M region relative to the DRI response and the scattering intensity of the 15° scattering angle is larger than that of the 90° scattering angle. It should be noted that light scattering intensities of this PP sample were much higher than those of the PS600k sample with a slightly lower M_w and narrower distribution. It was because the scattering intensity of the polymer was proportional to the product of C, M and $(dn/dc)^2$, while the absolute dn/dc value of PP was higher than PS in TCB at 150 °C (0.097 versus 0.053 ml/g), a PP molecule would have a much higher scattering intensity than PS molecule with the similar C and M.

Logarithms of M and R_g as functions of V_R for PP in TCB at 150 °C were shown in Fig. 9. The M and R_g averages of PP were calculated by the absolute calibration curves, which were established by lineally regression of the middle section of the data points and extrapolation to both ends. It should

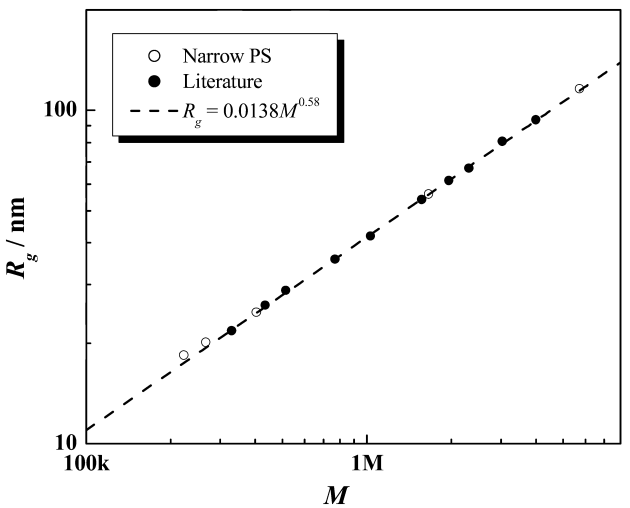

Fig. 6. R_{gu} as a function of M_w for narrow PS standards in TCB at 150 °C.

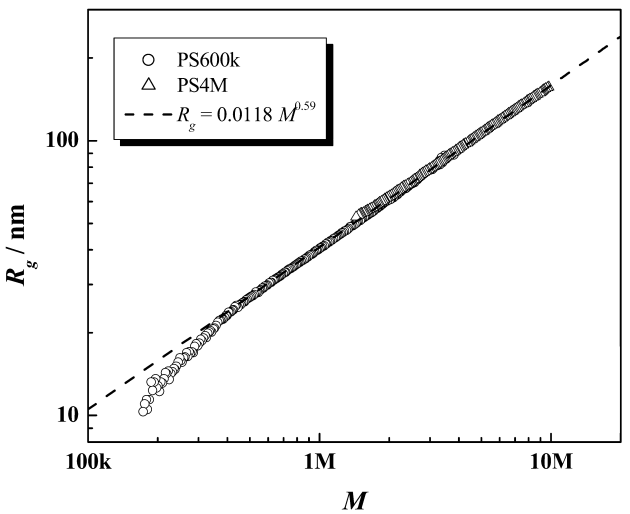

Fig. 7. R_g as a function of M for PS4M and PS600k in TCB at 150 °C.

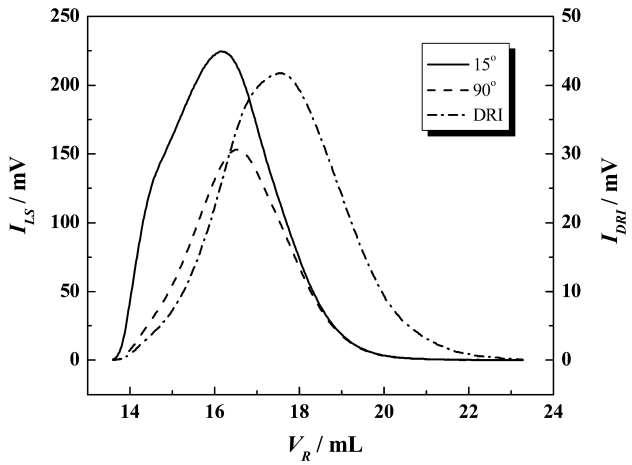

Fig. 8. GPC-TALLS chromatograms of PP in TCB at 150 °C.

be noted that the obtained R_{gi} were between 156 and 17 nm. The software was designed to calculate R_g between 10 and 150 nm, the extremely high molecular tail of this PP sample had exceeded the upper R_g limit of the software and can't be calculated. However, it can be extrapolated to both ends to calculate the averages. The calculated M and R_g averages of PP, as well as a HDPE sample, were summarized in Table 2.

The scaling relationship between R_g and M for HDPE and PP were shown in Fig. 10. An exponent of 0.56 was obtained for both samples, indicating the studied HDPE and PP took a random coil in TCB, a good solvent, at 150 °C. A lower intercept was observed for PP than HDPE, due to the effect of short chain branching on the size of polyolefin [14]. It should be noted that the studied HDPE reached both the low R_g limit of 10 nm and the high R_g limit of 156 nm of the

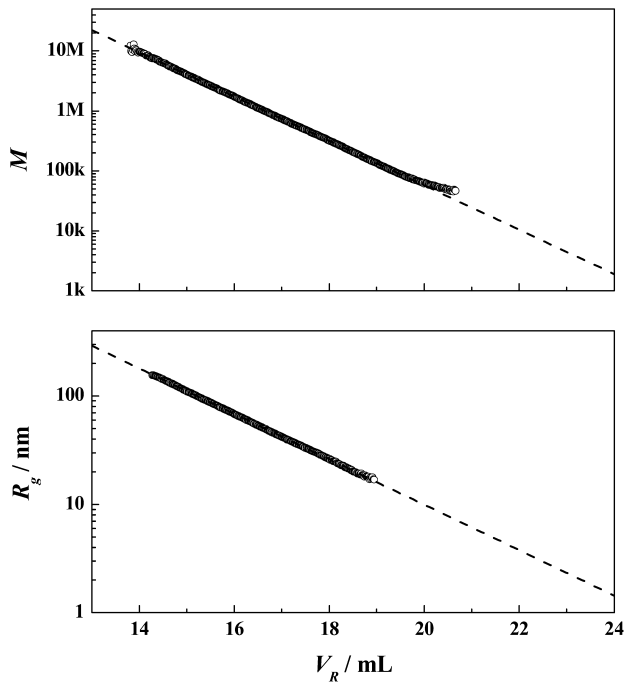

Fig. 9. Logarithms of M and R_g as functions of V_R for PP in TCB at 150 °C.

Table 2
M and R_g averages of PP and HDPE

Sample	M_n (k)	M_w (k)	M_z (k)	M_w/M_n	R_{gn} (nm)	R_{gw} (nm)	R_{gz} (nm)
PP	188	838	2376	4.45	20.7	47.3	84.1
HDPE	17.4	160	913	9.16	7.0	24.2	62.6

detector since it had a much broad MWD ($M_w/M_n = 9.2$) covering these size range with enough concentration.

4.3. PDMS

Fig. 11 showed a typical plot of the GPC-TALLS/DLS chromatograms of PDMS in TCB at 150 °C (with $C_{inj} = 2.70$ mg/ml). Similar trends of the SLS and DRI detector responses were observed with the above PS600k and PP sample, except that much higher intensities were shown for this PDMS sample. It was observed that the absolute intensities of the SLS detector response of this PDMS sample were about 10 times of those of the PS600k. However, they had a similar M_w and M_w/M_n (see Table 3), as well as a close C_{inj}, the difference was due to the absolute dn/dc value of PDMS was about 3 times of that of PS in TCB at 150 °C (0.153 versus 0.053 ml/g). In addition, DLS data were obtained for this PDMS sample with such a high scattering intensity. The collected $R_{h,app}$ decreased with V_R since GPC separated polymers according to their hydrodynamic volume in solution.

Logarithms of M, as well as R_g and R_h, as functions of V_R for PDMS in TCB at 150 °C were shown in Fig. 12. The absolute calibration curves of M, R_g and R_h, were established by lineally regression of the middle section of the data points and extrapolation to both ends. It was observed that the obtained R_h had a random uncertainty of 5%. However, the true $R_h - V_R$ relationship can be obtained

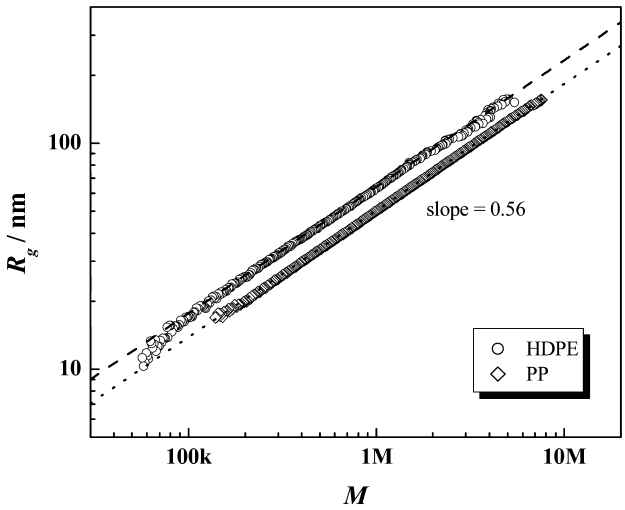

Fig. 10. R_g as a function of M for HDPE and PP in TCB at 150 °C. The broken line and the dot line indicate $R_g(\text{nm}) = 0.0280\,M^{0.56}$ for HDPE and $R_g(\text{nm}) = 0.0220\,M^{0.56}$ for PP, respectively.

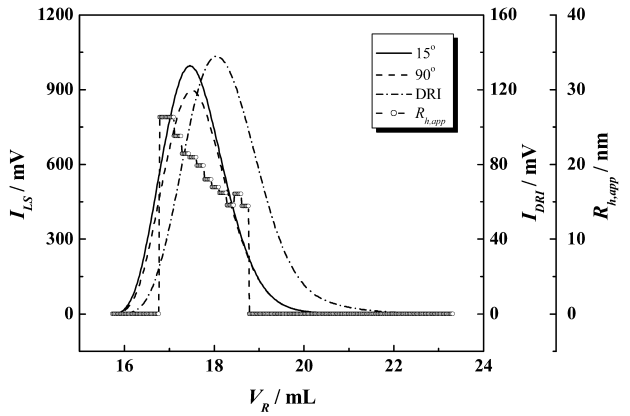

Fig. 11. GPC-TALLS/DLS chromatograms of PDMS in TCB at 150 °C.

by averaging the results of multiple runs. It was also consistent with the batch-mode DLS results of the same sample, which will be discussed later. The average properties of PDMS were calculated according to Eqs. (12)–(20) and the results were summarized in Table 3. The ρ-ratio ($\rho = R_{gz}/R_{hz}$), which reflects the architecture and conformation of polymers in solution, was calculated to be 1.48, which was much lower than the theoretical value for polydisperse linear random coil in good solvent (2.05) or in θ solvent (1.73) [10], indicating a compact coil conformation of PDMS in TCB at 150 °C.

The ρ-ratio was also calculated for PDMS fraction at each elution slice. The high performance columns used here ensured a very narrow distribution in both molecular weight and molecular sizes for each elution slice. The dependence of ρ-ratio on M can be conveniently obtained by comparing R_g and R_h data, which were obtained simultaneously for the same PDMS fraction eluted from the GPC columns. For fractions with M less than 500 k ($R_g < 20$ nm), R_g calculated from the absolute calibration curves in Fig. 12 was used because the measured R_g for small molecules had large uncertainty. The ρ-ratio kept an invariant value of 1.27 with a deviation of 5%, as shown in Fig. 13. It was much lower than the theoretical ρ-ratio for monodisperse linear random coil in good solvent (1.78) or in θ solvent (1.50) [10], indicating a compact coil conformation of PDMS in TCB at 150°. It was observed that PDMS did not fully dissolved in TCB until the temperature rose to 144 °C, TCB is not a good solvent for PDMS at 150 °C, thus the PDMS chain took a compact conformation, resulting a lower ρ-ratio than 1.50. Burchard et al. [15] and Wu et al. [16] had

Table 3
M, R_g and R_h averages of PDMS

	n-average	w-average	z-average
M (k)	319	641	965
R_g (nm)	16.2	23.1	28.3
R_h (nm)	7.7	14.4	19.2
ρ	–	–	1.48

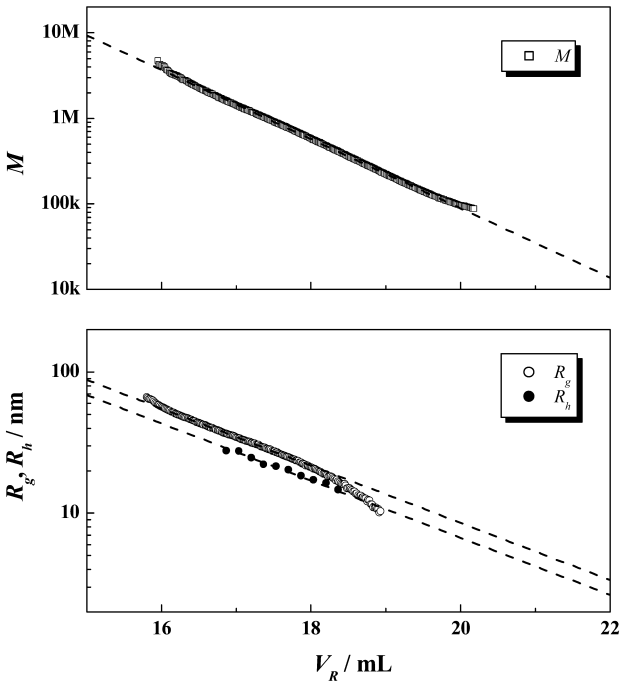

Fig. 12. Logarithms of M, R_g and R_h as functions of V_R for PDMS in TCB at 150 °C.

also obtained ρ-ratio less than 1.50 for different polymer coil in a not very good solvent.

The absolute R_g and R_h distributions of PDMS were obtained using the calibration curves in Fig. 12 and the DRI response, as presented in Fig. 14. A shift of R_h distribution against R_g distribution in the whole size distribution was observed, which agreed with the ρ-ratio of 1.27. Mrkvickova et al. had compared the size distribution data from DLS and SEC for PS in toluene and also observed such a shift with the exception of the lowest sizes where DLS becomes insensitive [17]. The flow-mode DLS in this study can provide a full R_h distribution compared with traditional

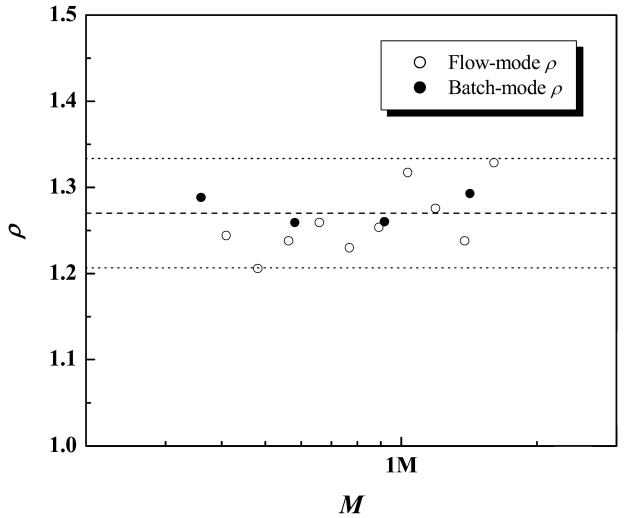

Fig. 13. ρ-ratio as a function of M for PDMS in TCB at 150 °C.

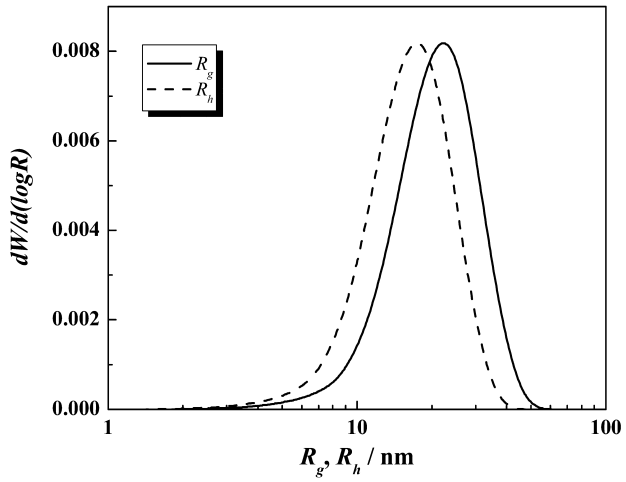

Fig. 14. Absolute R_g and R_h distributions of PDMS.

DLS, which often underestimated the small size molecules [18]. In addition, R_g and R_h data were obtained simultaneously for the same polymer fraction eluted from the GPC columns in this study, avoiding the laborious fractionation and following characterization work by SLS and DLS, respectively.

The scaling relationship between R_g, R_h and M for PDMS were shown in Fig. 15. The middle portion of the R_g–M plot was linearly fitted to obtain the scaling law. The relations of $R_g(\text{nm}) = 0.0250\,M^{0.51}$ and $R_h(\text{nm}) = 0.0196\,M^{0.51}$ were established for PDMS in TCB at 150 °C. Both R_g and R_h had a lower exponent of 0.51, indicating that PDMS took a compact coil conformation in TCB, a not very good solvent, at 150 °C, which agreed with the results from ρ-ratio.

The GPC-TALLS/DLS technique was proved to be a convenient and quick method to study the shape and conformation of polymers in solution, especially for those samples that were difficult to be characterized under normal

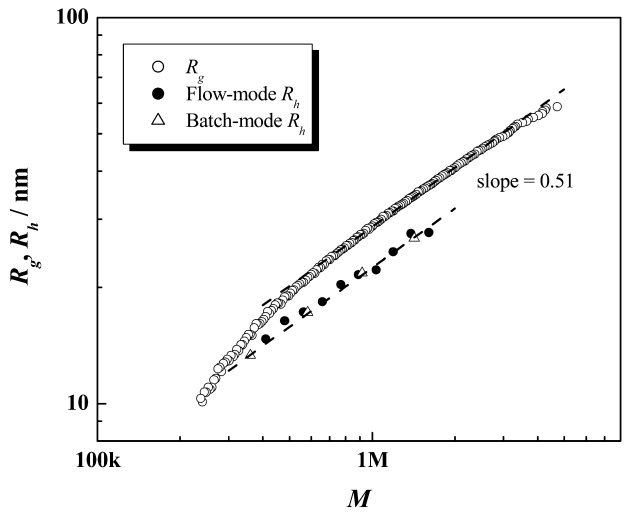

Fig. 15. R_g and R_h as functions of M for PDMS in TCB at 150 °C. The broken lines indicate $R_g(\text{nm}) = 0.0250\,M^{0.51}$ (upper) and $R_h(\text{nm}) = 0.0196\,M^{0.51}$ (lower) respectively.

condition, such as samples only dissolved in solvent at high temperature. It should be pointed out that flow-mode DLS is only applicable for high molecular weight polymers with a higher *dn/dc* value. Even for PDMS with a higher *dn/dc*, it only works in the middle portion of the chromatogram with M ranging from 400 k to 2 M. For PS and polyolefin with a lower *dn/dc* value, flow-mode DLS will only work for those sample with molecular weight higher than a few million.

As we had indicated above, the accumulation time was only 10 s with 5 μs sampling time for each R_h data in Fig. 11, one may question its reliability. The stop-flow GPC-TALLS/DLS experiments were performed in order to study the precision and accuracy of the results obtained in flow-mode DLS.

Fig. 16 showed the stop-flow GPC-TALLS/DLS chromatograms of PDMS in TCB at 150 °C (with $C_{inj} = 2.50$ mg/ml), the eluent flow was stopped at $V_R = 17.5$ ml. The accumulation time was 30 s with 10 μs sampling time for the DLS detector. Firstly, both LS and DRI detector responses did not change anymore after the eluent flow was stopped, indicating that the PDMS fraction with $V_R = 17.5$ ml. was successfully trapped in the LS flow cell. Secondly, the trapped fraction had a $R_{h,app} = (21.0 \pm 0.3)$ nm, showing good precision. It should be noted that the polymer concentration at $V_R = 17.5$ ml, which was calculated from the DRI response and the injected weight of the PDMS sample, was only 0.19 mg/ml.

Thus the flow-mode DLS detector served as a traditional batch-mode DLS detector after the eluent flow was stopped at a special time to trap the fraction wanted. And time correlation function was accumulated for different accumulation time to study its effect on the results obtained. Fig. 17 showed the normalized intensity–intensity time correlation function $|g^{(1)}(t)|^2$ for PDMS fraction with $V_R = 17.5$ ml, which were obtained at different accumulation time of 10, 60 and 600 s, respectively. As the accumulation time increased from 10 to 600 s, the obtained time correlation function became smoother since the signal-to-noise ratio increased with the experiment duration. The time

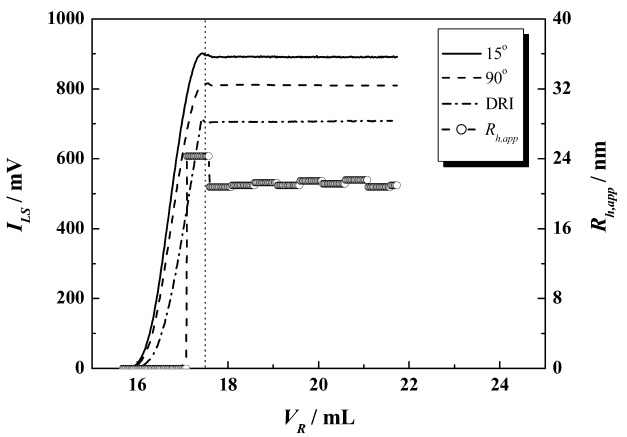

Fig. 16. Stop-flow GPC-TALLS/DLS chromatograms of PDMS in TCB at 150 °C.

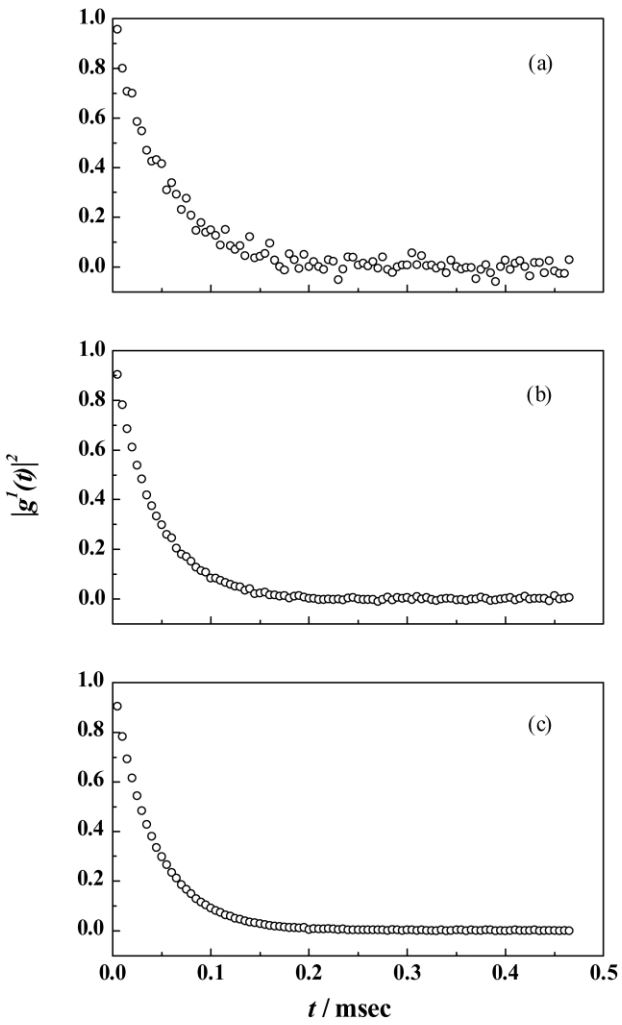

Fig. 17. Normalized intensity–intensity time correlation function $|g^{(1)}(t)|^2$ for PDMS fraction with $V_R = 17.5$ ml at different accumulation time of 10 s (a), 60 s (b) and 600 s (c).

correlation function accumulated at 600 s was rather accurate and the $R_{h,app}$ obtained thereby was regarded as the true value. Although there was more fluctuation for data obtained at a shorter accumulation time, the results obtained at different accumulation time were identical. As shown in Table 4, most of the obtained $R_{h,app}$ had a precision (standard deviation of $R_{h,app}$ expressed as percentage of average obtained by multiple runs, s/a) and accuracy (difference between average and true value of $R_{h,app}$ expressed as percentage, d) within 5%, even for those with accumulation time of only 10 s. An exception was the fraction eluted at $V_R = 18.5$ ml, the obtained $R_{h,app}$ at accumulation time of 10 s had a larger deviation due to the insufficient scattering intensity of the fraction with a lower M, as we had previously discussed. However, as the accumulation time increased to 60 or 600 s, an accurate $R_{h,app}$ was obtained. That is to say, for fraction with not so strong scattering intensity, one can still obtain an accurate DLS data by increasing the accumulation time. It was encouraged for other samples with a less scattering intensity, e.g., PS and polyolefin. It should also be noted that $R_{h,app}$ obtained from batch-mode and flow-mode DLS at accumulation time of 10 s were also identical in precision and accuracy, indicating the DLS detector saw the same fraction in the LS cell in both stop and flow state with the same quality.

Pecora had indicated that there is a practical limit for accurate DLS study of polymer when the light scattered by the solvent ($I_{solvent}$) is roughly equal in intensity to that scattered by the solute (I_{solute}) [5]. The light scattered by the solvent or the solution was recorded as number of photons received by the photodetector per sec. The molecular parameters, as well as the scattering intensity for PDMS fractions trapped at different V_R were summarized in Table 5. The ratio between scattering intensity of the solute to the solvent, $I_{solute}/I_{solvent}$, was calculated for each fraction.

Table 4
Precision and accuracy for $R_{h,app}$ of PDMS fractions at different V_R obtained in batch-mode and flow-mode DLS

V_R (min)		Batch-mode $R_{h,app}$ (nm) at accumulation time			Flow-mode $R_{h,app}$ (nm)
		600 s	60 s	10 s	
17.0	$a \pm s$[a]	$25.5^6 \pm 0.2^1$	$25.3^4 \pm 0.3^2$	$25.2^7 \pm 1.4^2$	$25.3^4 \pm 1.4^6$
	s/a[b] (%)	0.8	1.3	5.6	5.8
	d[c] (%)	–	−0.9	−1.1	−0.9
17.5	$a \pm s$	$21.1^3 \pm 0.0^4$	$21.1^5 \pm 0.2^7$	$22.0^0 \pm 0.7^1$	$21.2^1 \pm 0.4^1$
	s/a (%)	0.2	1.3	3.2	1.9
	d (%)	–	0.1	4.1	0.4
18.0	$a \pm s$	$16.9^3 \pm 0.0^6$	$16.9^1 \pm 0.2^2$	$16.4^5 \pm 0.8^8$	$17.2^3 \pm 0.5^5$
	s/a (%)	0.4	1.3	5.3	3.2
	d (%)	–	−0.1	−2.8	1.8
18.5	$a \pm s$	$13.2^0 \pm 0.3^0$	$13.0^8 \pm 0.7^4$	$12.9^6 \pm 1.0^0$	$15.0^2 \pm 1.2^6$
	s/a (%)	2.3	5.7	7.7	8.4
	d (%)	–	−0.9	−1.8	13.8

[a] Average ± standard deviation of $R_{h,app}$ obtained by multiple runs.
[b] Standard deviation expressed as percentage of average.
[c] Difference between average and $R_{h,app}$ obtained at accumulation time = 600 s.

Table 5
Molecular parameters and scattering intensity for PDMS fractions trapped at different V_R

V_R (min)	C[a] (mg/ml)	M[b] (k)	R_g[b] (nm)	$R_{h,app}$[c] (nm)	R_h[d] (nm)	$I_{solvent}$ (photons/s)	$I_{solution}$ (photons/s)	$I_{solute}/I_{solvent}$[e]
17.0	0.11	1424	34.8	25.6	26.8	1.23×10^5	1.96×10^5	0.59
17.5	0.22	924	27.5	21.1	21.8	1.23×10^5	2.46×10^5	1.00
18.0	0.26	585	21.7	16.9	17.2	1.23×10^5	2.12×10^5	0.72
18.5	0.22	363	17.2	13.2	13.4	1.23×10^5	1.70×10^5	0.38

[a] C was calculated from the DRI response for each V_R of the same sample with $C_{inj} = 2.70$ mg/ml.
[b] M and R_g were calculated from the absolute calibration curves in Fig. 12.
[c] $R_{h,app}$ was obtained from batch-mode DLS with accumulation time = 600 s.
[d] R_h was calculated from Eq. (11) with $f = 0.1$.
[e] $I_{solute}/I_{solvent} = (I_{solution} - I_{solvent})/I_{solvent}$.

Although the concentration of the trapped fraction at each V_R was very low (0.1–0.3 mg/ml), the light scattered by the solute was still high enough to perform an accurate DLS measurement in a rather short time. Compared the order of $I_{solute}/I_{solvent}$ with the data in Table 4, it showed that at the same accumulation time, the larger the ratio $I_{solute}/I_{solvent}$, the more precise and accurate the obtained $R_{h,app}$ was.

Fig. 18 showed the normalized intensity–intensity time correlation function $|g^{(1)}(t)|^2$ for PDMS fraction with V_R = 17.0, 17.5, 18.0 and 18.5 ml at accumulation time of 600 s. It showed that the fraction with a lower V_R had a larger delay time, since it had a larger size.

According to Stokes–Einstein equation, the transitional diffusion coefficient (D) of PDMS was calculated from its R_h for each fraction and the correlation between D and M was established. Fig. 19 showed the relation between D and M for PDMS in TCB at 150 °C and $D\,(cm^2/s) = 3.21 \times 10^{-4} M^{-0.51}$ was established.

5. Conclusions

Both absolute molecular weight and molecular sizes of polymers, including PS, PE, PP and PDMS, eluting from the GPC columns were obtained simultaneously using an on-line TALLS/DLS detector. The absolute molecular weight and molecular sizes distributions of these polymers were obtained. However, it was found that flow-mode DLS was only applicable for high molecular weight polymers with a higher *dn/dc* value such as PDMS, due to the extremely dilute concentration of polymer eluting from the GPC columns and the short accumulation time of DLS data.

The scaling relationship between R_g and M was obtained despite the column dispersion, which provided information on polymer conformation in solution. The values of the exponents in scaling laws was found to be 0.59 for PS and 0.56 for HDPE and PP, indicating these polymers took a random coil conformation in TCB, a good solvent, at 150 °C.

The relations of $R_g(nm) = 0.0250\,M^{0.51}$ and $R_h(nm) = 0.0196\,M^{0.51}$ were established for PDMS in TCB at 150 °C. Both R_g and R_h had a lower exponent of 0.51, and ρ-ratio was found to be 1.27, indicating PDMS took a compact coil conformation in TCB, a not very good solvent, at 150 °C. The relation of $D\,(cm^2/s) = 3.21 \times 10^{-4}\,M^{-0.51}$ was established for PDMS in TCB at 150 °C.

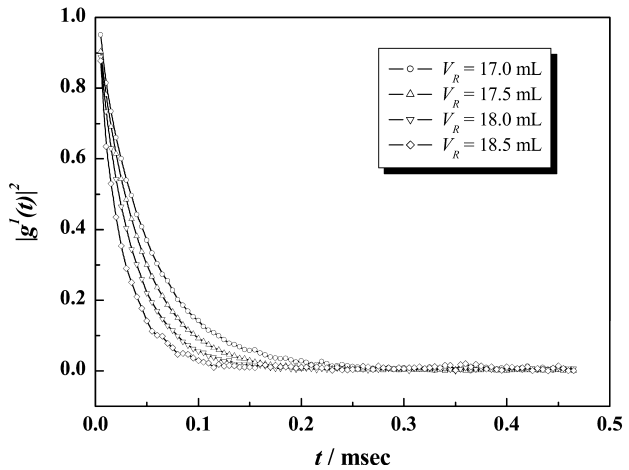

Fig. 18. Normalized intensity–intensity time correlation function $|g^{(1)}(t)|^2$ for PDMS fraction with V_R = 17.0, 17.5, 18.0 and 18.5 ml at accumulation time of 600 s.

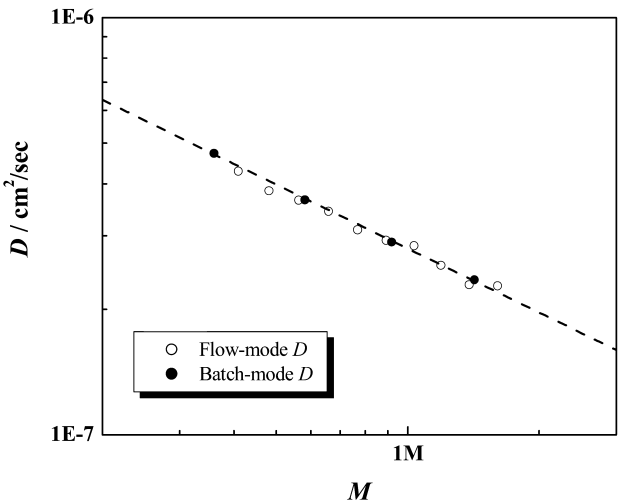

Fig. 19. D as a function of M for PDMS in TCB at 150 °C.

The DLS results obtained for PDMS in flow-mode agreed well with those obtained in batch-mode for the same PDMS sample. The GPC-TALLS/DLS technique was proved to be a convenient and quick method to study the shape and conformation of polymers in solution at high temperature, especially for those samples that were difficult to be characterized under normal condition.

Acknowledgements

This work was subsidized by the Special Funds for Major State Basic Research Projects of China and supported by the State Key Laboratory of Polymer Physics and Chemistry of China.

References

[1] Jeng L, Balke ST, Mourey TH, Wheeler L, Romeo P. J Appl Polym Sci 1993;49:1359–74.
[2] Mourey TH, Coll H. J Appl Polym Sci 1995;56:65–72.
[3] Podzimek S. J Appl Polym Sci 1994;54:91–103.
[4] Chu B. Laser light scattering. New York: Academic Press; 1991.
[5] Pecora R. Dynamic light scattering. New York: Plenum Press; 1985.
[6] Helfrich JP. Am Biotech Lab 1998;16:64–6.
[7] Frank R, Frank L, Ford NC. In: Provder T, Barth HG, Urban MW, editors. Chromatographic Characterization of Polymers: Hyphenated and Multidimensional Techniques. Adv Chem Ser 247, Washington, DC: American Chemical Society; 1995. p. 109–21.
[8] Stockmayer WH, Schmidt M. Pure Appl Chem 1982;54:407–14.
[9] Huber K, Burchard W, Fetters LJ. Macromolecules 1984;17:541–8.
[10] Burchard W. Adv Polym Sci 1999;143:113–94.
[11] He Z, Zhang X, Cheng R. J Liq Chromatogr 1982;5:1209–22.
[12] Kasparkova V, Ommundsen E. Polymer 1993;34:1765–7.
[13] De Gennes PG. Scaling concepts in polymer physics. Cornell University Press: Ithaca, NY; 1979.
[14] Sun T, Brant P, Chance RR, Graessley WW. Macromolecules 2001; 34:6812–20.
[15] ter Meer HU, Burchard W, Wunderlich W. Colloid Polym Sci 1980; 258:675–84.
[16] Zhang G, Wu C. J Am Chem Soc 2001;123:1376–80.
[17] Mrkvickova L, Porsch B, Sundelof LO. J Appl Polym Sci 1995;58: 2033–8.
[18] Wu C, Lilge D. J Appl Polym Sci 1993;50:1753–9.